Journal of Ceramic Processing Research. Vol. 23, No. 3, pp. 397~403 (2022)
(Received 29 January 2022, Received in revised form 14 February 2022, Accepted 8 April 2022)
https://doi.org/10.36410/jcpr.2022.23.3.397

J O U R N A L O F
Ceramic Processing Research

Effect of cryogenic treatment on nitinol alloy reinforced with mwcnt and its effect on high temperature wear analysis

V. Kavitha[a,*], R. Soundararajan[b] and V. Senthil[c]
[a]*Assistant Professor, Mechanical Engineering, RVS College of Engineering and Technology, Coimbatore, Tamilnadu, India*
[b]*Associate Professor, Mechanical Engineering, Sri Krishna College of Engineering and Technology, Coimbatore, Tamilnadu, India*
[c]*Associate Professor, Mechanical Engineering, Coimbatore Institute of Technology, Coimbatore, Tamilnadu, India*

Nickel-Titanium (NiTi) is a material adopted in modern manufacturing sectors as its super elastic nature and shape memory behaviour provides unique properties that can be integrated into complex applications and designs. The present investigation focused on understanding the effects of cryogenic treatment composites i.e. Nickel-Titanium (nitinol) alloy reinforced with Multi-Wall Carbon Nanotubes (MWCNT). The novel nitinol of $[49Ni\text{-}51Ti]_{100\text{-}x}$ – X wt.% MWCNT (X = 0.5, 1.0, and 1.5) were fabricated using Powder metallurgy technique. The fabricated samples were characterized using Optical Microscope (OM), Scanning Electron Microscope (SEM), Energy Dispersive Spectroscopy (EDS), and X-Ray diffraction spectroscopy (XRD). Further, the fabricated samples were cryogenically treated at a temperature of -77 K in a liquid nitrogen atmosphere. The optical microstructural analysis result shows uniform distribution of MWCNT particles. The cryogenic treated samples were subjected to analyse the hardness and high-temperature wear properties. The result clearly portrays that cryogenic treated samples improves the hardness and high temperature wear behaviour significantly compare to the non-cryogenic treated samples. The investigation of mechanical properties result shows that cryogenic treated sample such as 47.5Ni-49.5Ti-1.5MWCNT achieves a higher hardness about 262 HV.

Keywords: cryogenic, MWCNT, Temperature, Wear, XRD

Introduction

Nickel-titanium alloys commonly called nitinol, a shape memory alloy (SMA), is recognized as an alloy for the next generation. It has been widely used in several applications such as biomedical, aerospace, actuators, automotive, and MEMS devices. Ni and Ti based super alloys were grown nowadays in the field of aerospace sectors. It has a distinctive property such as excellent hardness, strength and good corrosion resistance. Many researchers are focused on the new material development for the aerospace inner casings. Moreover, Ni-Ti alloys are widely used in numerous trades due to its subsequent properties like well corrosion resistance and machinability properties [1].

However, the combination of Ni and Ti is called Nitinol having equiatomic proportions and subsequently it's having excellent mechanical and tribological properties in the area of shape memory alloys. Nitinol displays high elasticity owing to its extensive recoverable strain range while at stress level is low. In specific, Ni-Ti alloys are used in the instrument which is for root canal preparation application [2, 3]. Some researchers are undergone the research in this area and recommends that Ni alloy content may release in an aggressive physiological in vivo environment and these types are Ni may persuade toxic and make allergic to the human body. During high temperature, the NiTi phase is termed as austenite and following that complex body-centered cubic crystal structure was formed. In reverse, at low temperature, martensite following that monoclinic crystal structure was formed. Fabrication of Ni-Ti based alloy microstructure can be fabricated by powder metallurgy and their performances were evaluated [4]. This process is widely accepted to manufacture Ti-Ni based alloy using main techniques like conventional sintering, high temperature synthesis, injection molding and laser melting etc. [5, 6]. During conventional sintering methods, Ti_2Ni phase and $TiNi_3$ precipitates were formed and it deteriorated the functional properties of the Ti-Ni alloy.

On the other hand, Nitinol (Ni-Ti) alloy has shape memory abilities and it reflects its shape memory effect and hyperelasticity. In this regard, it is widely used in medical industries such as orthodontic arch wire, implants and heart stents. When the Nitinol is placed in a multifaceted physiological atmosphere containing corrosive electrolytic solution, the surface morphology, mechanical and physical properties will change and it reduces the clinical value and upsetting its service function and time. Many researchers are undergoing

*Corresponding author:
Tel : +91 8903961416
E-mail: vkavithagunasekaran@gmail.com

their research in the area of functional and mechanical properties evaluation. Pfeifer et al. [7] studied the utilization of the functional properties of shape memory alloys and showed that it had adaptable orthopaedic implants and it can alter the properties as the healing occurs. Reclaru et al. [8] and Tarnita et al. [9] reported that shape memory alloys have several advantages in specific modular patient specific models. However, it is less expensive to manufacture the component and provides the ability to utilize it in multi metals. Wang et al. [10] described the mechanical behaviour of shape memory alloy, tensile strength is significant one but the characteristics such as temperature transformation, and residual stresses under both the loaded conditions are considered into account. However, with the Ni-Ti alloy fusion welding method, many disadvantages are there such as formation of coarse grain microstructure in the melt pool. It reduces the properties of shape memory alloys. Frenzel et al. [11], Elahinia et al. [12] deliberate that the NiTi temperature transformation is very complex as composition changes. At 1 wt.% of nickel content could change the entire results of shape memory alloys and temperature transformation at almost 100 ^{o}C.

Very limited work was involved in high temperature wear analysis of the Ni-Ti based alloy under cryogenic treatment. There forth, the current study is focused on to evaluate the high temperature wear behaviour of 49 Ni-51 Ti alloy reinforced with MWCNT with varying the wt.% such as 0.5, 1.0 and 1.5. The fabricated composites were characterized using Optical Microscope (OM), Scanning Electron Microscope (SEM), Energy Dispersive Spectroscopy (EDS) and X-Ray diffraction analysis (XRD). After sample preparation, the samples were cryogenically treated at -77 K temperature in a liquid nitrogen atmosphere. After cryogenic treatment, the samples were undergone hardness and high temperature wear analysis using tribo apparatus. Afterward, the worn surface of the worn samples was assessed using SEM.

Investigational Procedure

In this study Ni, Ti and MWCNT was acquired from M/S. Alfa Acear, USA. Ni, and Ti particle sizes are around 44 μm in size and the MWCNT diameter was 20 nm and the height of the nanotube was 50 μm respectively. Initially, 49Ni-51Ti was prepared as wt.% basis following that ball milling was acquired. 0.5%, 1.0% and 1.5 wt.% of MWCNT was mixed with the Ni-Ti alloy using a ball milling process. While increasing the wt.% of the MWCNT, subsequently, Ni and Ti particles wt.% was reduced. The following four samples were prepared using powder metallurgy technique namely 49Ni-51Ti, 48.5Ni-50.5Ti-0.5MWCNT, 48Ni-50Ti-1MWCNT and 47.5Ni-49.5Ti-1.5MWCNT.

Cold compaction and Sintering

After ball milling, the composite powders were cold compacted using a compression testing machine having the pressure of 20 MPa. After compaction, the samples were sintered using Muffle Furnace at the temperature of 900 ^{o}C at inert atmosphere. After sintering, the samples were polished using a polishing testing machine for 1 hr. to obtain a better surface.

Afterwards, the samples were cryogenically treated at -77 K in the liquid nitrogen environment. The hardness of the samples was evaluated using Vickers Hardness. The high temperature wear behaviour of the samples was evaluated using pin-on-disc apparatus at the temperature range of 30 ^{o}C, 50 ^{o}C, 100 ^{o}C, 150 ^{o}C and 200 ^{o}C. After wear analysis, the sample surfaces were assessed using SEM. The detailed analysis is deliberated in subsequent sections.

Results and Discussion

Microstructural and Phase Angle Evaluation

Figs. 1(a & b) shows the optical microscope image of cryogenic treated samples such as 49Ni-51Ti and 47.5Ni-49.5Ti-1.5MWCNT. Before cryogenic treatment,

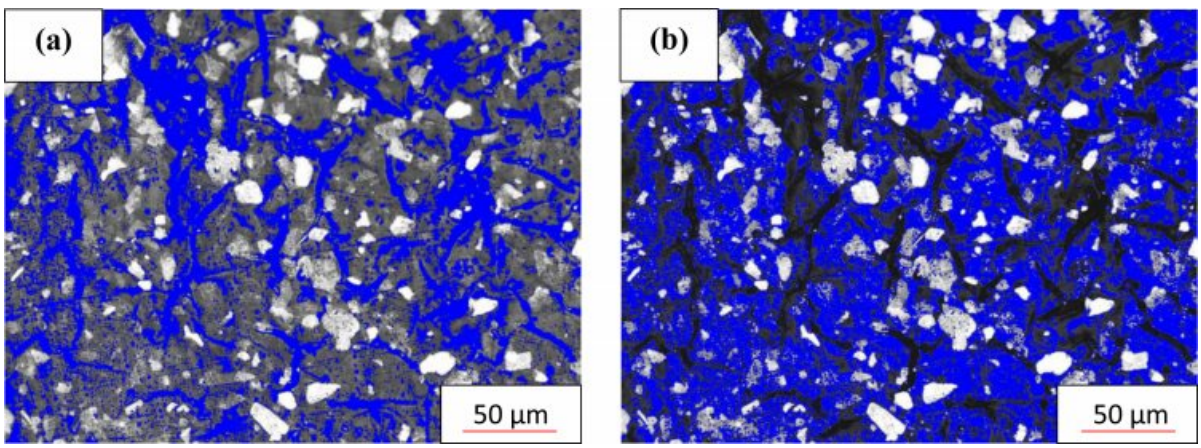

Fig. 1. Optical Microscope image of cryogenic treatment: (a) 49Ni-51Ti and (b) 47.5Ni-49.5Ti-1.5MWCNT.

the NiTi phase was termed as austenite and following that complex body-centered cubic crystal structure was formed. In reverse, at low temperature, martensite following that monoclinic crystal structure was formed and displayed in Figs. 1(a & b). The careful observation was also made on the cryogenic treatment samples using SEM. Figs. 2(a & b) shows the SEM images of 49 Ni-51 Ti and 47.5Ni-49.5Ti-1.5MWCNT treated samples and it illustrates that the secondary particles are evenly distributed in the matrix (49Ni-51Ti). Following that the elemental confirmation was assessed using Energy Dispersive Spectroscopy (EDS) analysis and exhibited in Figs. 3(a & b). From Figs. 3, the presence of Ni, Ti and MWCNT are confirmed. Before and after treatment, no reaction occurred; further the grain structure was changed from austenite to martensite.

Figs. 4(a & b) shows the XRD analysis of Ni-Ti and Ni-Ti-MWCNT composites and it illustrates that amorphous phase was identified for Ni-Ti alloy and crystalline phase was viewed while reinforcing MWCNT in the Ni-Ti alloy. However, the miller indices of Ni, Ti and MWCNT are (111) (200) , (220) & (101), (111), (220) & (002) (100). It was confirmed by the JCPDES no. JCPDS no. 04-0835, 44-1294 and 96-101-1061.

Evaluation of Vicker's Hardness

The Vickers hardness of the fabricated samples before treatment and after treatment was assessed and the corresponding graph was shown in Fig. 5. From the Fig. 5, it clearly evident that after treatment the hardness was increased irrespective of samples. On the other hand, while increasing the wt.% of MWCNT, again the hardness of the samples was increased. 47.5Ni-49.5Ti-1.5MWCNT after treatment shows better hardness. This is happening, because during treatment NiTi phase has been termed as martensite following that monoclinic crystal structure was formed [13-18]. This will increase the hardness of the sample invariably.

High Temperature wear rate analysis

After treatment, all the samples were undergone high temperature wear analysis at the temperature range of 30 ºC, 50 ºC, 100 ºC, 150 ºC and 200 ºC. As for as concern of the temperature, all the samples possessed higher wear rate for both the cases before and after

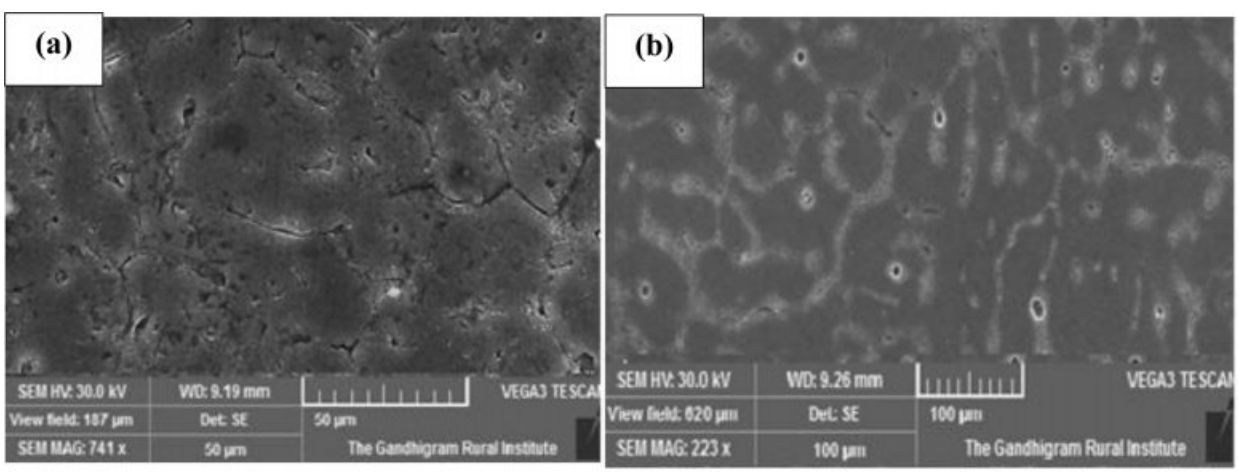

Fig. 2. SEM image of cryogenic treatment: (a) 49Ni-51Ti and (b) 47.5Ni-49.5Ti-1.5MWCNT.

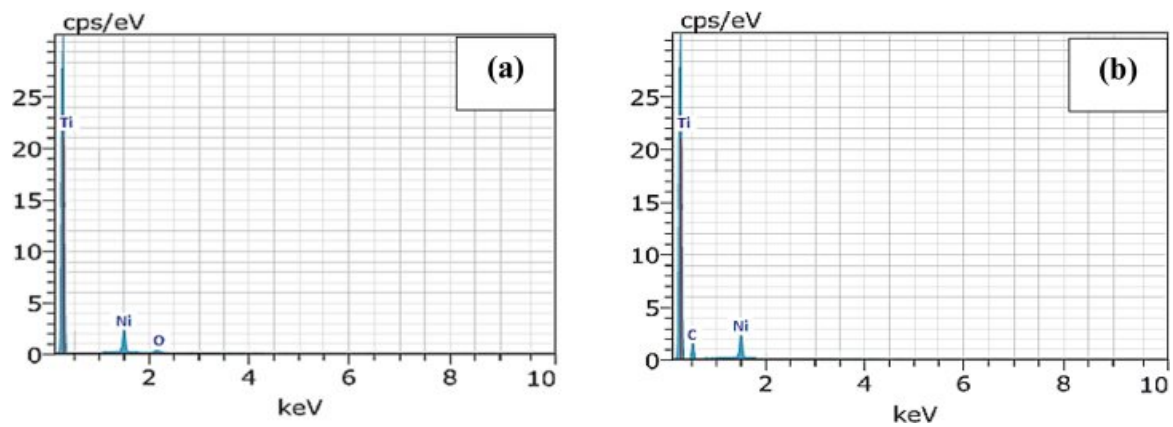

Fig. 3. EDS spectrum of cryogenic treated samples: (a) 49Ni-51Ti and (b) 47.5Ni-49.5Ti-1.5MWCNT.

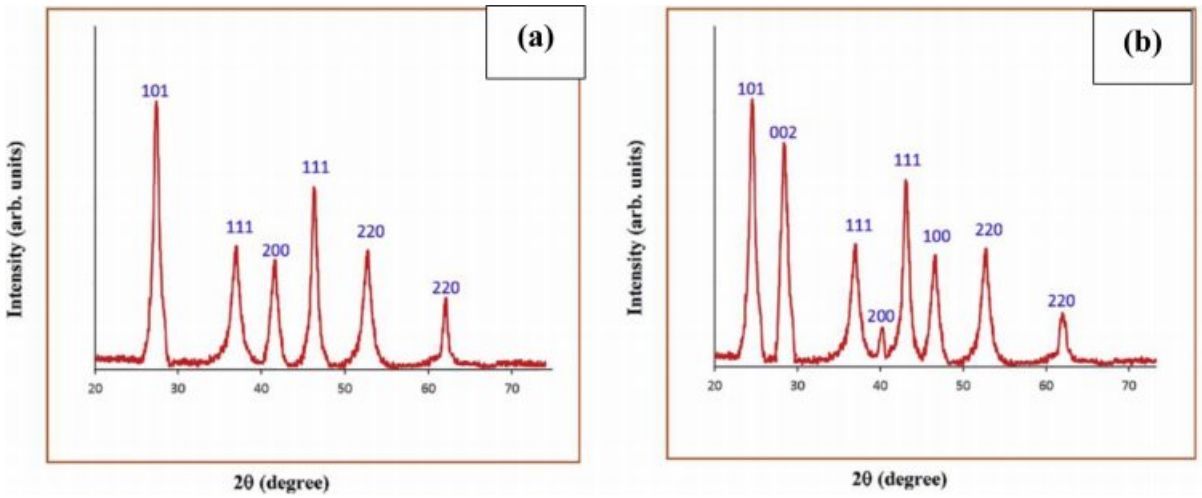

Fig. 4. XRD analysis of cryogenic treated samples: (a) 49Ni-51Ti and (b) 47.5Ni-49.5Ti-1.5MWCNT.

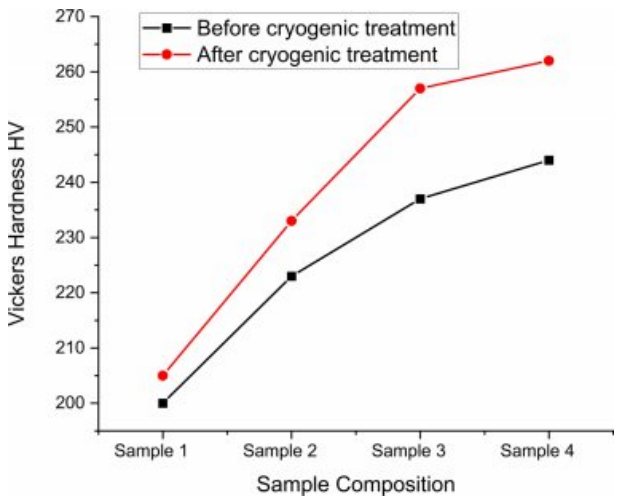

Fig. 5. Vickers hardness of the fabricated Ni-Ti based alloy before and after cryogenic treatment.

treatment and as shown in Figs. 6(a and b). Initially, the steady state time will take to obtain the required temperature. During wear test, the sample temperature will again increase because of the interaction between the samples and the beside part. According to Fig. 6(b) at all temperature conditions, the wear rate was increased irrespective of the treatment condition and the sample composition. Also observed that 47.5Ni-49.5Ti-1.5MWCNT after treatment achieves lower wear rate when compared to other samples. Fig. 6(a) shows the wear rate of the composites, for different loading conditions. While increasing the load, the wear rate of the composite is also increased irrespective of the treatment and sample condition. This was happening because after treatment, the grain structure will get coarsen and it displays an extensive recoverable strain range at stress level which is low. However, the environment is also acting a vital role during sliding [19-23]. While experimentation, a huge amount of oxide was formed on the specimen surface and it acted as a defensive layer for the samples. It reduces the wear rate in all conditions. On the other hand, after cryogenic treatment, the grain structure will get refined, and the distance between the two grains gets closer. It also influences the performance of wear property.

High Temperature coefficient of friction

After treatment, all the samples were undergone high temperature wear analysis at the temperature range of 30 ºC, 50 ºC, 100 ºC, 150 ºC and 200 ºC. As for as concern of the temperature, all the samples possessed higher coefficient of friction for both the cases before and after treatment and as shown in Fig. 7(a and b). Initially, the steady state time will take to obtain the required temperature. During the wear test, the sample temperature will again increase because of the interaction between the samples and the counterpart. According to Fig. 7(b) at all temperature conditions, the coefficient of friction was increased irrespective of the treatment condition and the sample composition. But 47.5Ni-49.5Ti-1.5MWCNT after treatment shows lower coefficient of friction, when compared to other samples. Fig. 7(a) shows the coefficient of friction of the composites, for different loading conditions. While increasing the load, the coefficient of friction of the composite is also increased irrespective of the treatment and sample condition [23]. This was happening because after treatment, the grain structure will get coarsen and it displays an extensive recoverable strain range at stress level and is low. However, the environment is also acting a vital role during sliding. While experimentation, a huge amount of oxide was formed on the specimen surface and it acted as a defensive layer for the samples. It reduces the coefficient of friction at all conditions.

Surface Morphology

Secondary electron images of worn surface analysis

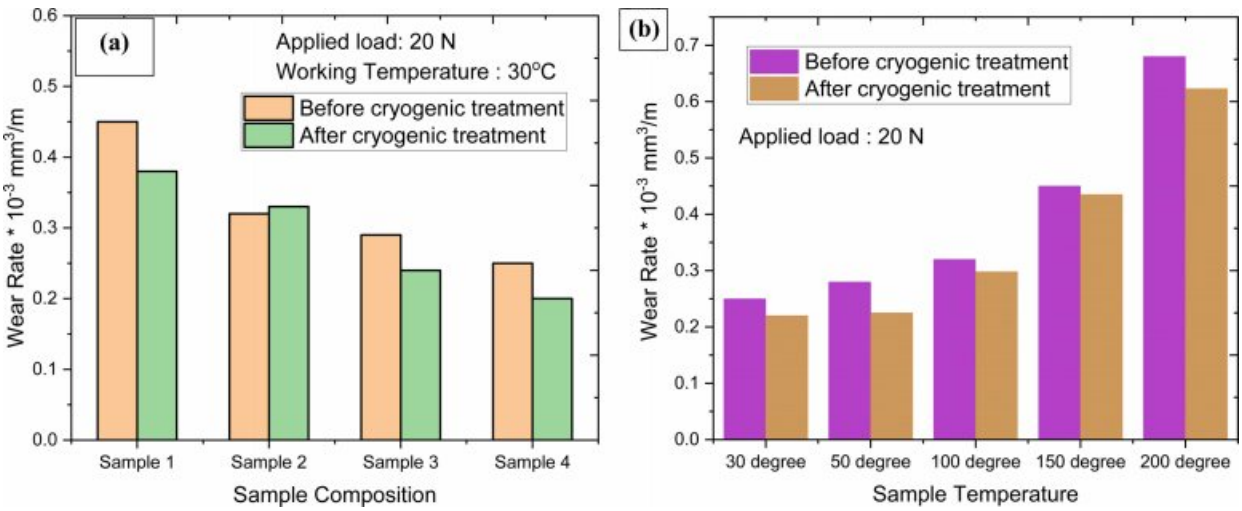

Fig. 6. High Temperature wear rate analysis: (a) based on sample composition and (b) based on sample temperature.

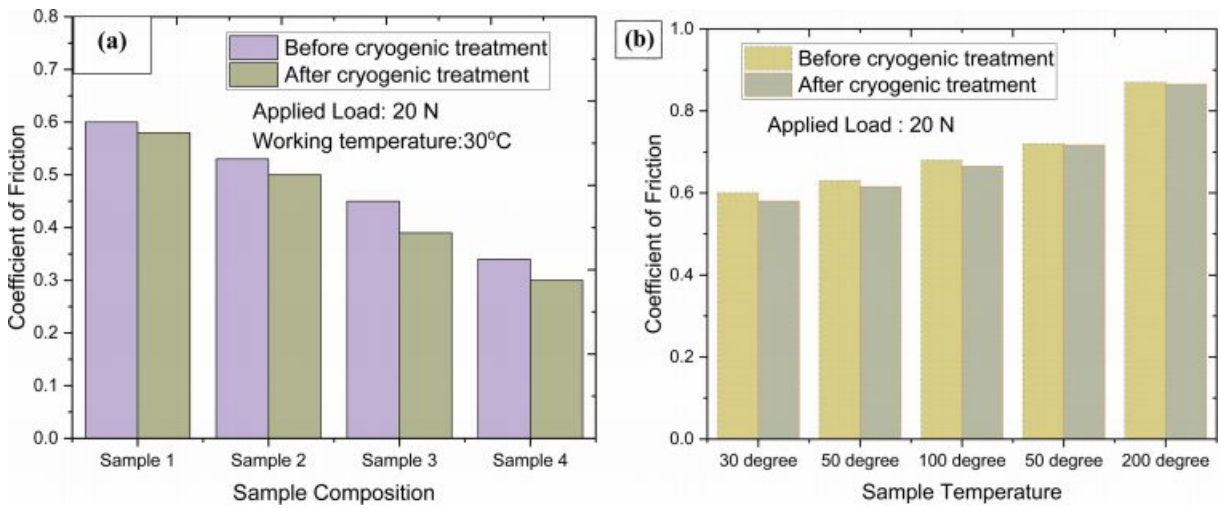

Fig. 7. High Temperature coefficient of friction analysis: (a) based on sample composition and (b) based on sample temperature.

for before and after treatment are displayed in Figs. 8(a-d). From Figs. 8(a and c), it illustrates that the present wear mechanisms which comprise crater, furrows and Spalling were observed before treatment. The wear degree was varied based upon the position. Under continual impacts, abrasive friction was created and it led to a plastic deformation of the un-treated samples becoming severe. Furthermore, many defects are derived in the sample surface such as microcracks and stress attention. It starts the material flow before work hardening. The wear experimentation will take place over a long period, it creates impact wear and it reaches the higher limit and hence the specimen surface layer is separate, which causes higher material loss. The entire un-treated area possessed a similar phenomenon in the worn morphologies which creates tiny furrows, flat hardened areas, visible cracks and Spalled areas. After treatment, some defects are noticed like pits and grooves and no evidence of material loss are observed during pits. The worn surface of 47.5Ni-49.5Ti-1.5MWCNT after treatment and 200 ºC temperature sample was assessed for further investigation. Fig. 8(d) displays the SEM images relating the worn surface of 47.5Ni-49.5Ti-1.5MWCNT after treatment and 200 ºC, the worn surface regime, shows some dark layers and structural deformation regime are observed on the surface [24]. The dark layer has a hardened layer and it is difficult to wear. This is an important phenomenon of the worn surface of Ni-Ti alloy after cryogenic treatment. Further increasing the sample temperature from 100 ºC to 200 ºC, some outermost layers are observed, which is called the second layer of oxide layer. It acts as a shielding of the sample and reduces surface wear. On the other hand, during experimentation, the initiation and expansion of the surface and oxide layer and also subsurface cracks is having a strong influencing parameter for material loss before treatment [25-27]. However, plastic deformation accrued endlessly over the period of time, which will

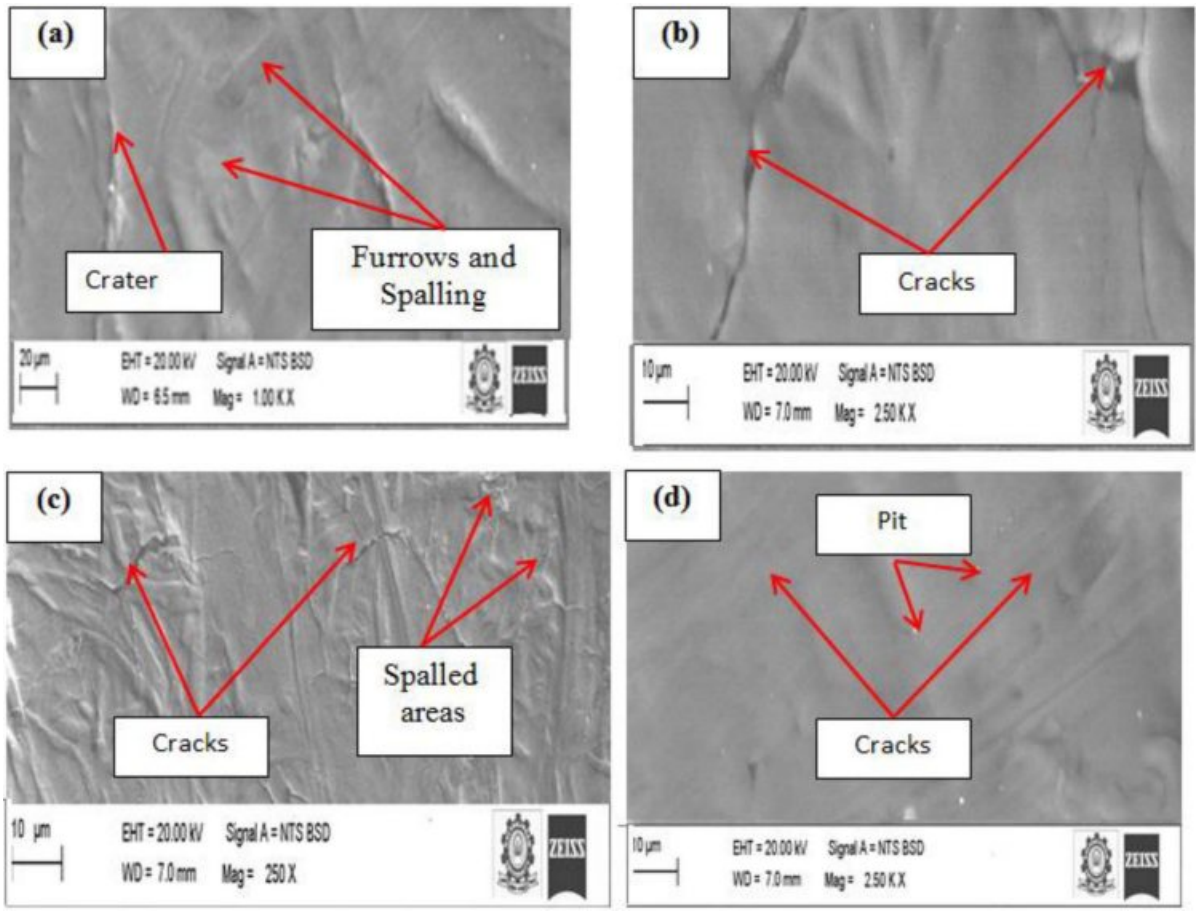

Fig. 8. surface morphology analysis of (a) 49Ni-51Ti before cryogenic treatment, (b) 49Ni-51Ti after cryogenic treatment at 30 ºC, (c) 47.5Ni-49.5Ti-1.5MWCNT before cryogenic treatment, and (d) 47.5Ni-49.5Ti-1.5MWCNT after cryogenic treatment at 200 ºC.

increase the sample hardness which is closely correlated with the Fig. 5 and it can reduce plasticity considerably.

Conclusion

Nickel-Titanium (nitinol) ([49Ni-51Ti] $_{100-x}$) alloy was reinforced with Multi Wall Carbon Nanotubes (MWCNT) at various wt.%– X wt.% MWCNT (X = 0.5, 1.0, and 1.5) using Powder metallurgy (P/M) technique. After composite fabrication, all the samples were cryogenic treated at -77K under liquid nitrogen atmosphere. The research results were revealed that after cryogenic treatment, the hardness of the samples was increased significantly and it reached maximum hardness up to 262 HV. Wear rate and coefficient of friction of the composites were increased irrespective of the treatment and sample condition because coarse grain structure was formed after cryogenic treatment. The cryogenic treated sample 47.5Ni-49.5Ti-1.5MWCNT at 100 ºC produces a structural deformation in surface regimes. Further increments of sample temperature from 100 ºC to 200 ºC, some outermost layers were observed which is called the second layer or oxide layer. The oxide layers act as a shielding for cryogenic treated sample 47.5Ni-49.5Ti-1.5MWCNT and reduces the surface to worn.

References

1. Z. Liu, X. Feng, X. Yi, K. Sun, H. Wang, Z. Gao, and X. Meng, Prog. Nat. Sci.: Mater. Int. 31 (2021) 749-754.
2. X. Cai, H. Li, B. Ji, M. Li, X. Yao, Y. Wang, and D. Sun, Opt. Laser Technol. 146 (2022) 107575.
3. X. Yi, H. Wang, K. Sun, W. Gao, B. Sun, G. Shen, X. Meng, Z. Gao, and W. Cai, J. Alloys Compd. 854 (2021) 157159.
4. T. Fukagawa, Y. Saito, and A. Matsuyama, J. Alloys Compd. 896 (2021) 163118.
5. O.O. Shichalin, I.Y. Buravlev, E.K. Papynov, A.V. Golub, A.A. Belov, A.A. Buravleva, V.N. Sakhnevich, M.I. Dvornik, N.M. Vlasova, A.V. Gerasimenko, V.P. Reva, and A.A. Yudakov, Int. J. Refractory Metals Hard Mater. 102 (2022) 105725.
6. J. Pang, Y. Xu, J. Tian, Y. Zhou, D. Xue, X. Ding, and J. Sun, Mater. Sci. Eng. A 807 (2021) 140850.
7. R. Pfeifer, C.W. Muller, C. Hurschler, S. Kaierle, V. Wesling, and H. Haferkamp, Procedia CIRP 5 (2013) 253-258.
8. L. Reclaru, R. Lerf, P.-.Y. Eschler, and J.-.M. Meyer, Biomaterials 22 (2001) 269-279.

9. D. Tarnita, D. Tarnita, and D. Bolcu, Biomed. Eng. (2011) 431-468.
10. W. Wang, X. Yang, H. Li, F. Cong, and Y. Liu, Adv. Mater. Sci. Eng. 2014 (2014) 1-8.
11. J. Frenzel, E.P. George, A. Dlouhy, C. Somsen, M.F.-X. Wagner, and G. Eggeler, Acta Materialia 58 (2010) 3444-3458.
12. M.H. Elahinia, M. Hashemi, M. Tabesh, and S.B. Bhaduri, Prog. Mater. Sci. 57 (2012) 911-946.
13. L. Jiang, X. Cui, G. Jin, H. Tian, Z. Tian, X. Zhang, and S. Wan, Appl. Surf. Sci. 575 (2022) 151645.
14. K. Ohno, M. Tsuchiya, R. Kuwahara, R. Sahara, S. Bhattacharyya, and T.N. Pham, Comput. Mater. Sci. 191 (2021) 110284.
15. Y.-M. Byoun, S.-K. Seo, J.-d. Yoon, and S.-J. Na, J. Ceram. Process. Res. 20 (2019) 556-562.
16. B. Gwalani, S. Shukla, D. Leonard, J. D. Poplawsky, D. T. Pierce, L. Kovarik, G. Muralidharan, and A. Devaraj, J. Alloys Compd. 886 (2021) 161207.
17. J. Li, K. Sun, Y. Jiang, X. Meng, and W. Cai, Mater. Lett. 293 (2021) 129732.
18. P. Li, Y. Jia, J. Yi, X. Ma, J. Pu, and D. Wang, J Alloys Compd. 844 (2020) 156175.
19. H. Nam and K.-W. Nam, J. Ceram. Process. Res. 22 (2021) 66-73.
20. G.S. Pandolfi, S.C. Martins, V.T.L. Buono, and L.A. Santos, J. Mater. Res. Technol. 9[4] (2020) 9162-9173.
21. P. Jiang, H. Huang, B. Sun, G. Song, W. Wu, Z. Wang, and Y. Zhang, Mater. Today Commun. 24 (2020) 101112.
22. S. Liu, C. Xia, T. Yang, Z. Yang, N. Liu, and Q. Li, Mater. Lett. 260 (2020) 126938.
23. J. Umar Mohamed, P.L. Palaniappan, P. Maran, and R. Pandiyarajan, J. Ceram. Process. Res. 22 (2021) 306-316.
24. İ. Topcu, J. Ceram. Process. Res. 22 (2021) 276-282.
25. G. Zhao, J. Chen, C. Ding, D. Fang, C. Huang, and X. Ye, Vacuum 177 (2020) 109381.
26. D.C. Ren, H.B. Zhang, Y.J. Liu, Shujun Li, W. Jin, R. Yang, and L.C. Zhang, Mater. Sci. Eng. A 771 (2020) 138586.
27. J.S. Kim, Y.J. Kim, W.C. Kim, W.T. Kim, and D.H. Kim, Intermetallics 124 (2020) 106867.